Eur. Phys. J. Appl. Phys. **90**, 10902 (2020)

https://doi.org/10.1051/epjap/2020190324

THE EUROPEAN PHYSICAL JOURNAL APPLIED PHYSICS

Regular Article

Acoustic demultiplexer based on Fano and induced transparency resonances in slender tubes★,★★

Abdelkader Mouadili[1], El Houssaine El Boudouti[2,*], and Bahram Djafari-Rouhani[3]

[1] LPMCER, Département de Physique, Faculté des Sciences et Techniques de Mohammedia, Université Hassan II, Casablanca, Morocco
[2] LPMR, Département de Physique, Faculté des Sciences, Université Mohammed I, Oujda, Morocco
[3] IEMN, UMR CNRS 8520, Département de Physique, Université de Lille, 59655 Villeneuve d'Ascq, France

Received: 6 November 2019 / Received in final form: 30 March 2020 / Accepted: 3 April 2020

Abstract. We give an analytical demonstration of the possibility to realize a simple phononic demultiplexer based on Fano and acoustic induced transparency resonances. The demultiplexer consists of a Y-shaped waveguide with an input line and two output lines. Each output line contains two stubs grafted either at a given position or at two positions far from the input line. We derive in closed form the expressions for a selective transfer of a single propagating mode through one line keeping the other line unaffected.

1 Introduction

Fano and EIT (Electromagnetically Induced Transparency) resonances [1–3] have an atomic origin, but they have been the subject of several studies in classical systems such as coupled micro-resonators [4–6], photonic waveguides [7–11], acoustic slender tube waveguides and solid-liquid multilayers [12–21] as well as plasmonic nonostructures [22–26]. Fano resonance can be explained as the product of two processes of constructive and destructive wave interferences. This phenomenon gives rise to a resonance followed by an antiresonance over a narrow frequency range and can be manifested by an asymmetrical profile shape. In the transmission spectra, the Fano profile appears as a maximum near to a transmission zero [27,28]. When the Fano resonance falls between two antiresonances (two transmission zeros) it becomes an EIT resonance. In optics this phenomenon has shown potential applications to realize slow light and data storage of optical information [29–32]. Fano and EIT resonances are originally the product of a coupling between one or more discrete states and a continuum [3].

In general, to create this type of resonances in classical systems, one directly or indirectly connects two or more resonators with a waveguide. Among the simple structures giving a clear theoretical and experimental demonstration of such resonances, one can cite a guide connected with two lateral resonators at the same position (called a cross structure) or at two different positions (called U-shaped structure). In acoustics the U-shaped structure was first studied by El Boudouti et al. [12] to show Fano and AIT (the acoustic analogue of EIT) resonances. A few years later, the same structure was studied by Santillan et al. [13] to demonstrate AIT resonances and delayed sound. More recently, cross and U-shaped structures have been the subject of interest by Merkel et al. [14] to experimentally show AIT and Fano resonances as well as the possibility to realize perfect absorption with such structures. Similar structures but with multiple stubs have been proposed by Long et al. [33] to realize multiband and broadband absorbers for low-frequency sound. One can also cite the earlier work of Robertson et al. [34] where the effect of a defect in slowing down the group velocity in a one dimensional acoustic band gap array was studied. It is worth mentioning that cross and U-shaped photonic structures based on coaxial cables have been studied both theoretically and experimentally [10,11] in the radio-frequency domain. In addition, the cross structure has been proposed to study a Y-shaped demultiplexer based on EIT resonances [35]. This demultiplexer consists on one input line and two output lines, each one containing a cross-shaped resonator.

Acoustic demultiplexers based on phononic crystals with different defects has been realized either through what is called add-drop filters [36,37] or multi-port channels [38,39]. Recently, three-port acoustic network has been used to study subwavelength control of absorption [40] using resonators on each channel. Also, it has been shown in multi-channel systems, the possibility to generate outgoing waves only in certain channels by controlling the incoming waves. Such systems, called coherent perfect channeling, have been demonstrated in three- and four-port configurations in presence of a resonator at the common junction. The incoming waves are first coherent perfectly channeled to other channels, in which they

★Contribution to the topical issue "Advanced Electromagnetic Materials and Devices (META 2019)", edited by A. Razek and S. Zouhdi.
★★ Supplementary material is available in electronic form at https://www.epjap.org/10.1051/epjap/2020190324
* e-mail: elboudouti@yahoo.fr

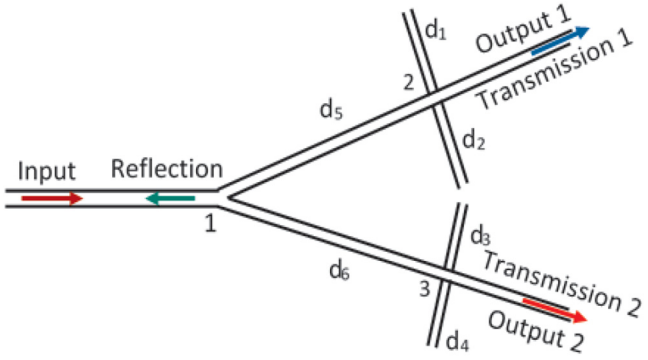

Fig. 1. Schematic representation of a Y-shaped demultiplexer with one input line and two output lines. Two stubs are grafted at the same position along each output line. The geometrical parameters are defined in the text.

could then be manipulated. If the manipulation is absorption, then the process will give rise to coherent perfect absorption [41]. In this paper we propose two Y-shaped acoustic demultiplexers with two different configurations: the first structure is based on the cross-shape structure (Fig. 1) and the second one is based on the U-shape structure (Fig. 7). The demultiplexers in these two devices are based on AIT and Fano resonances. Our objective consists of demonstrating the possibility of finding analytically the appropriate lengths of the different waveguide resonators in order to reach total transmission in one output line keeping the other lines unaffected. The demultiplexers proposed in this study have several advantages over those based on phononic crystals [38,39], such as: i) the simplicity of the device manufacturing where only two resonators are needed on each output line instead of a periodic structure with a given defect, ii) the simplicity of the structure enables a full analytical calculation which allows to deduce the exact expressions of the different lengths of the waveguides to achieve a perfect demultiplexing. iii) The possibility of increasing the quality factor of the filtered resonances to infinite values by detuning the lengths of the two stubs. This property is a feature of Fano and induced transparency resonances that does not exist in standard phononic crystals with defects in which filtering is performed using finite width Breit-Wigner resonances [34,38,39,42]. It should be pointed out that the validity of our results is subject to the requirement that the cross section of the slender tubes being negligible compared to their length and to the propagation wavelength. The assumption of monomode propagation is then satisfied.

The rest of the paper is organized as follows: in Section 2 we shall give the analytical expressions of the lengths of the tubes that enables to realize a perfect demultiplexing for the cross structure. These analytical results are obtained from an analysis of the transmission and reflection coefficients and will be illustrated by numerical applications in standard acoustic slender tubes [13]. Section 3 gives the same results as in Section 2 but for U-structure. The last section contains the concluding remarks.

2 Demultiplexer based on cross structure

2.1 Transmission and reflection coefficients

Consider the structure shown in Figure 1, this structure is composed of an input line and two output lines, all fixed at point 1. The first output line contains two stubs of lengths d_1 and d_2 inserted on the same site 2 at a distance d_5 from the input 1. Likewise, the second output line contains two stubs of lengths d_3 and d_4 inserted on the same site 3 at the distance d_6 from the input 1. The possibility of realizing an AIT type resonance in a simple cross structure composed of two resonators of lengths d_1 and d_2 connected at one point along an infinite waveguide, has been the subject of several previous works [12–14]. In a cross structure, the AIT resonance is obtained by the entire stub of lengths $d_0 = d_1 + d_2$. This resonance is trapped between two transmission zeros induced by the two elementary stubs of length d_1 and d_2.

The calculation of the transmission and reflection coefficients is carried out using the Green's function method [43]. For simplicity, all waveguides are assumed being characterized by the same characteristic impedance $Z = \frac{\rho v}{S}$ where $\rho = 1.2\,\mathrm{Kg/m^3}$ and $v = 342\,\mathrm{m/s}$ are respectively the density and velocity of the fluid inside the slender tubes (namely, air) and $S = 3.14\,\mathrm{cm^2}$ is the section of the guide. We have chosen the same parameters as those used in the experimental work by Santillan and Bozhevolnyi [13]. However, the resonators are supposed to be simple stubs instead of Helmholtz resonators with narrow neck in order to get analytical expressions for a perfect demultiplexing (see below), otherwise the calculation becomes cumbersome and only numerical simulation can be performed.

The analytical expressions of the transmission coefficients t_1 and t_2 along first and second output lines and the reflection coefficient r in the input line are obtained using the same procedure of calculation as for photonic waveguides [35]. We shall avoid the details of these calculations (see the supplementary material[1]) and give below the expressions of t_1, t_2 and r in closed form, namely

$$t_1 = \frac{2C_1C_2(-C_6C_3C_4 + S^{'}S_6 + jC_3C_4S_6)}{\chi_1 + j\chi_2}, \quad (1)$$

$$t_2 = \frac{2C_3C_4(-C_5C_1C_2 + SS_5 + jC_1C_2S_5)}{\chi_1 + j\chi_2}, \quad (2)$$

and

$$r = -\frac{\xi_1 + j\xi_2}{\chi_1 + j\chi_2} \quad (3)$$

where

$$\xi_1 = C_1C_2C_3C_4(S_5S_6 - C_5C_6) + C_1C_2S^{'}C_6S_5 + C_3C_4SC_5S_6 + SS'S_5S_6 \quad (4)$$

[1] The supplementary material gives the details of the Green's function calculations to derive all the transmission and reflection coefficients.

$$\xi_2 = C_1C_2C_3C_4S_0 + C_1C_2S^{'}C_5C_6 + C_3C_4SC_5C_6 - S_0SS^{'} \quad (5)$$

$$\chi_1 = 3C_1C_2C_3C_4(S_5S_6 - C_5C_6) + C_1C_2S'(S_0 + C_5S_6) + C_3C_4S(S_0 + C_6S_5) - SS'S_5S_6 \quad (6)$$

$$\chi_2 = C_1C_2C_3C_4(3C_6S_5 + 3C_5S_6) + (C_5C_6 - 2S_5S_6)(C_1C_2S' + C_3C_4S) - S_0SS^{'} \quad (7)$$

and $C_i = \cos(kd_i)$, $S_i = \sin(kd_i)$ (i = 1-6), $S = \sin(k(d_1 + d_2))$, $S^{'} = \sin(k(d_3 + d_4))$, $S_0 = \sin(k(d_5 + d_6))$. $k = \omega/v$ is the wave-vector of the sound wave in the slender tubes and ω is the angular frequency.

In the absence of loss, the transmission coefficients in the two output lines are given respectively by $T_1 = |t_1|^2$ and $T_2 = |t_2|^2$ while the expression of the reflection R in the input line is given by $R = |r|^2$. The transmission and reflection coefficients satisfy the energy conservation: $T_1 + T_2 + R = 1$.

2.2 Numerical results and discussions

Now, we are able to choose the precise parameters of the system to obtain a complete transmission in the two output lines with neighboring frequencies. Indeed, from equations (1), (2) and (3), one can show easily that in order to realize $|T_1| = 1$, $T_2 = 0$ and $R = 0$, one should have $C_3C_4 = 0$ (i.e., $C_3 = 0$ or $C_4 = 0$), $S = 0$ and $C_6 = 0$. Similarly, in order to realize $|T_2| = 1$, $T_1 = 0$ and $R = 0$, one should have $C_1C_2 = 0$ (i.e., $C_1 = 0$ or $C_2 = 0$), $S' = 0$ and $C_5 = 0$. Now, in order to realize both $T_1 = 1$ and $T_2 = 1$ at two different and neighboring frequencies, we can show after some algebraic calculations that the six lengths d_1, d_2, d_3, d_4, d_5 and d_6, should satisfy the following conditions:

$$d_1 = \frac{d_0}{2} - \frac{\delta}{2} \quad (8)$$

$$d_2 = d_5 = \frac{d_0}{2} + \frac{\delta}{2} \quad (9)$$

$$d_3 = d_6 = \frac{d_0}{2} \quad (10)$$

$$d_4 = \frac{d_0}{2} + \delta, \quad (11)$$

where we have introduced a detuning parameter $\delta = d_2 - d_1 \neq 0$ between the two stubs along the output 1 (Fig. 1). This is a necessary and sufficient condition to realize an AIT resonance along the output 1. In addition, along this study we shall fix the length of the two stubs (i.e., $d_0 = d_2 + d_1$) which fixes the position of the AIT resonance along the output 1.

In order to illustrate the results above, we present in Figure 2 the variation of the transmission coefficients T_1 and T_2 and the reflection coefficient R as a function of the frequency f for different values of $\delta = d_2 - d_1$ around $\delta = 0$ and for $d_0 = 8.57$ cm. The choice of the length of $d_0 = d_1 + d_2$ enables to fix the frequency of the first AIT resonance induced by the two stubs along the first output at $\omega d_0/v = \pi$ (i.e., around $f_0 = 2000$ Hz as in reference [13]). Similarly, the length of the two stubs along the second line $d_0' = d_3 + d_4$ is chosen such that the second resonance induced by the later stubs falls at the vicinity of the one induced by the former stubs. In particular, we have chosen the same parameter δ representing the detuning between the AIT resonances and at the same time the separation between the transmission zeros of each AIT resonance (i.e., $d_0' - d_0 = d_2 - d_1 = d_4 - d_3 = \delta$).

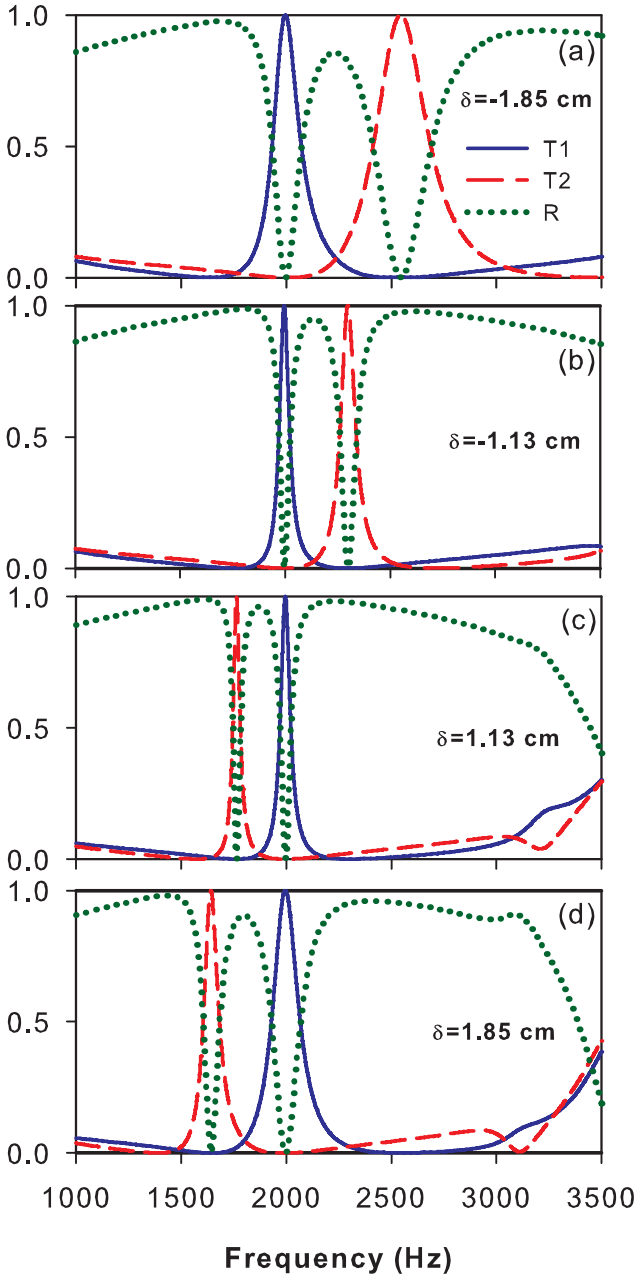

Fig. 2. Variation of the transmission along the output 1 (continuous curve), the output 2 (discontinuous curve) and the reflection in the input (dotted curve) of the demultiplexer as a function of frequency f for different values of $\delta = d_2 - d_1$ and for $d_0 = d_1 + d_2 = 8.57$cm.

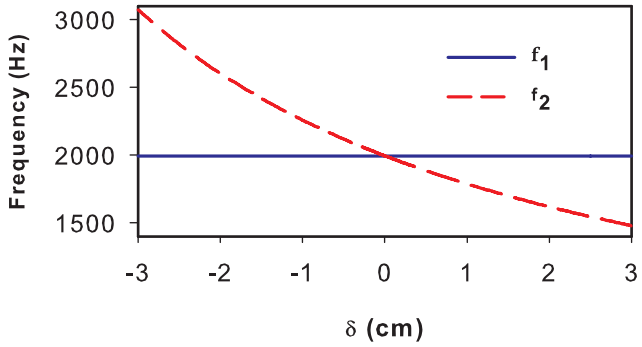

Fig. 3. Variation of the frequency of the two AIT resonances along the two output guides as a function of δ.

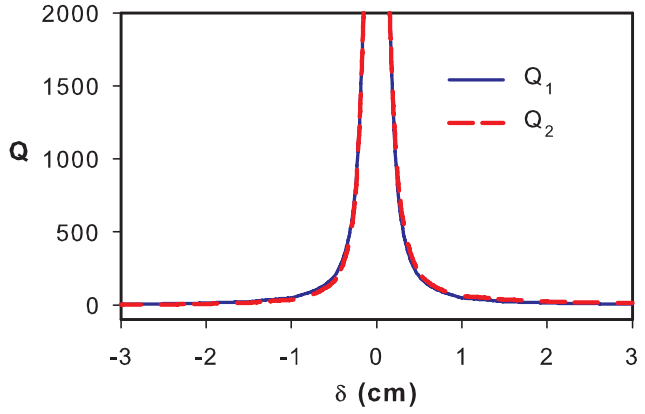

Fig. 4. Variation of the quality factors Q_1 and Q_2 of the AIT resonances as a function of δ.

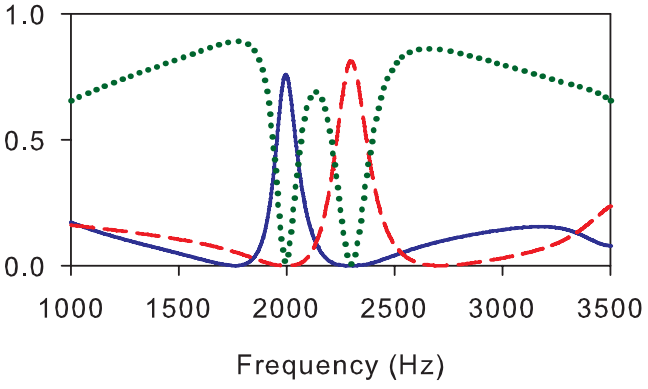

Fig. 5. Same as in Figure 2b but in presence of loss in the slender tubes.

Figure 2 clearly shows that when the transmission along the first output (continuous curve) reaches unity ($T_1 = 1$), the transmission along the second output T_2 (discontinuous curve) and the reflection R (dotted curve) vanish (i.e., $T_2 = R = 0$). Similarly, when the transmission along the second output line (discontinuous curve) reaches unity ($T_2 = 1$), the transmission along the first output line T_1 (continuous curve) and the reflection R (dotted curve) vanish (i.e., $T_1 = R = 0$). As mentioned above, the AIT resonance in the first output falls at the same frequency $f_0 \simeq 2000\,\text{Hz}$ for all δ values, its width decreases when δ decreases and disappears for $\delta = 0$ (Fig. 2). In addition, the shape and width of the AIT resonance changes slightly when δ becomes negative (i.e., for a permutation of both stubs 1 and 2). The position and width of the resonance along the second line strongly depend on δ. Indeed, since the first resonance AIT has two transmission zeros around $f_0 = 2000\,\text{Hz}$, the position of the second AIT resonance falls above $f_0 = 2000\,\text{Hz}$ for $\delta < 0$ (Figs. 2a and 2b), crosses the first resonance at $\delta = 0$ and reappears below $f_0 = 2000Hz$ for $\delta > 0$ (Figs. 2c and 2d). This is illustrated in Figure 3 where we have given the variation of the frequencies f_1 and f_2 of both resonances for different values of δ. It can be noted that the frequency f_1 of the resonance along the first line remains constant at f_0 regardless the value of δ, whereas the frequency f_2 of the second resonance falls above f_0 for δ negative ($\delta < 0$) then it reappears below f_0 when δ becomes positive ($\delta > 0$). The crossing between the two resonances takes place for $\delta = 0$.

Figure 4 gives the quality factor Q of the two resonances as a function of δ. We remark that the quality factor is almost the same for both resonances; it decreases very rapidly as a function of δ and tends to infinity when δ tends to zero. This kind of resonance (with infinite lifetime) is called *bound in continuum state* [44], it represents a stationary mode in the cross stubs and do not interact with the incident waves in the main waveguides.

In the previous results we have neglected the effect of loss on the AIT resonances. In Figure 5 we have given the same transmission spectra as in Figure 2b but in presence of damping. We have considered the same damping due to viscosity and thermal conduction in the resonators as in the experimental work by Santillan and Bozhevolnyi [13]. One can see that the transmission does not reach unity because of the attenuation of sound in the guides, the energy transmitted remains less than 80% in both branches. Also, the effect of absorption on the amplitude of the AIT resonances becomes very important for resonances with narrow width.

In order to analyze the spatial localization of the different modes that can be filtered or stopped by the demultiplexer, we have calculated the displacement field along the two output lines of the system [43]. Figure 6 gives the square modulus of the displacement field $|U|^2$ for the resonance $f_1 = 2000\,\text{Hz}$ with $\delta = -1.85\,\text{cm}$, i.e., $d_1 = 5.21\,\text{cm}$, $d_2 = d_5 = 3.36\,\text{cm}$, $d_3 = d_6 = 4.285\,\text{cm}$, $d_4 = 2.435\,\text{cm}$ (Fig. 2a). This mode corresponds to a filtered mode (full curve) in one line and a stopped mode (dashed curve) in the other line (Fig. 2a). Figure 6 shows that the mode $f_1 = 2000\,\text{Hz}$ is transferred along the output 1 (Fig. 6a), whereas it is stopped along the output 2 (Fig. 6b). The transfer of this mode along the output 1 is due to the excitation of both stubs of lengths d_1 and d_2 along this line as it illustrated in Figure 6c, whereas its stopping along the second line is due to the excitation of the stationary mode of only the stub of length $d_4 = 2.435\,\text{cm}$ as shown in Figure 6d. Similar results are obtained for the resonance mode $f_2 = 2544\,\text{Hz}$, but this time the transfer occurs along the second line through the excitation of its double stubs of lengths d_3 and d_4, whereas

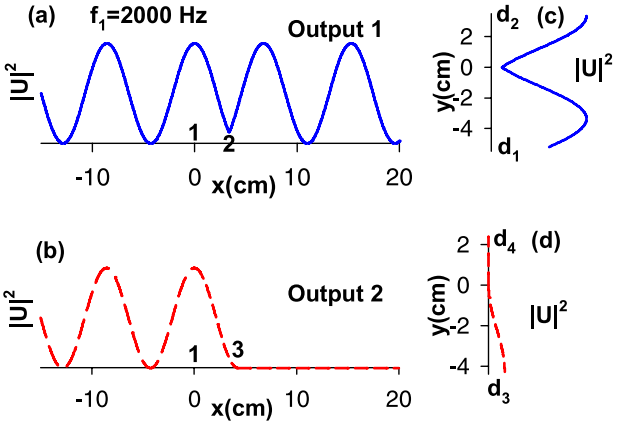

Fig. 6. Square modulus of the displacement field $|U|^2$ (in arbitrary units) versus the space position along the output 1 (a) and the output 2 (b) for $f_1 = 2000Hz$. (c) and (d) show the behavior of $|U|^2$ along the vertical stubs in each line. 1, 2 and 3 indicate the entrance and the exit along each line (Fig. 1)

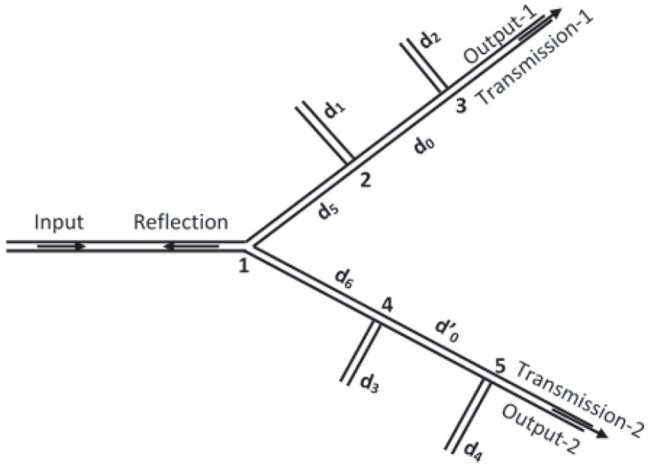

Fig. 7. Schematic representation of a Y-shaped demultiplexer with one input line and two output lines. Two stubs are grafted at two different positions along each output line. The geometrical parameters are defined in the text.

the wave is stopped along the first line as a consequence of the excitation of the mode of one of its stubs of length $d_2 = 3.36\,\text{cm}$. These results clearly show how the lengths of the finite guides constituting the demultiplexer should be chosen appropriately in order to transfer a wave in one line keeping the other line unaffected.

3 Demultiplexer based on U-structure

As mentioned above, the U-shaped resonator along a waveguide was the subject of several studies in acoustics by different authors [12,14]. In particular, it was shown that such structures can present two types of resonances: AIT-type resonances when the two resonators have different lengths and Fano resonances when the two resonators have the same lengths. In this section we consider the U-shaped demultiplexer composed of an input line and two output lines, all connected at the same point 1 (Fig. 7). On the first output line we connect two lateral stubs of lengths d_1 and d_2 separated by a distance d_0. The stub of length d_1 is inserted in the site 2 at a distance d_5 from the input 1 and the stub of length d_2 is inserted in the site 3 at a distance $d_5 + d_0$ from input 1. Similarly, the second output line contains two lateral stubs of lengths d_3 and d_4 separated by a distance d'_0. The stub of length d_3 is inserted in the site 4 at the distance d_6 from the input 1 and the stub of length d_4 is inserted in the site 5 at a distance $d_6 + d'_0$ from the input 1 (Fig. 7).

The calculation of the transmission and reflection coefficients for the demultiplexer based on U-shaped structure can be performed in the same way as in Section 2 using the Green's function method [43] (see the supplementary material[1]). However, the corresponding expressions are more cumbersome; therefore, we shall give only the conditions that should be satisfied by all the guides in order to realize perfect demultiplexing. Also, we shall distinguish two different cases depending on whether the stubs along each output line are slightly different which gives rise to AIT resonances or identical which gives rise to Fano resonances.

3.1 Demultiplexer based on AIT resonances

As already demonstrated in previous works [12,14], in order to get AIT resonance with such structures, we should take the lengths of the two stubs along one guide slightly different (i.e., $\delta = d_2 - d_1 \neq 0$). In addition, along this study we will fix the total length of the two stubs along the first output line such that $d_0 = d_2 + d_1$ which fixes the position of the AIT resonance along this line. Now, in order to achieve total transmission for two neighboring frequencies along the two output lines, the lengths of the different guides should be taken as follows:

$$d_1 = \frac{d_0}{2} + \frac{\delta}{2}, \tag{12}$$

$$d_2 = d_5 = \frac{d_0}{2} - \frac{\delta}{2}, \tag{13}$$

$$d_3 = d_6 = \frac{d_0}{2}, \tag{14}$$

$$d_4 = \frac{d_0}{2} - \delta, \tag{15}$$

$$d'_0 = d_3 + d_4 = d_0 - \delta. \tag{16}$$

Figure 8 presents the variation of the transmission coefficients T_1 and T_2 and the reflection coefficient R as a function of the frequency f for different values of δ around $\delta = 0$. We can see clearly that for each δ, when the transmission along the first output line (continuous curve) reaches unity ($T_1 = 1$), the transmission along the second output line T_2 (discontinuous curve) and the reflection R (dotted curve) cancel out each other (i.e., $T_2 = R = 0$). Similarly, when the transmission along the second line (discontinuous curve) reaches unity ($T_2 = 1$), the transmission along the first line T_1 (continuous curve) and the reflection R (dashed curve) vanish (i.e., $T_1 = R = 0$). As mentioned above, the AIT resonance in the first output

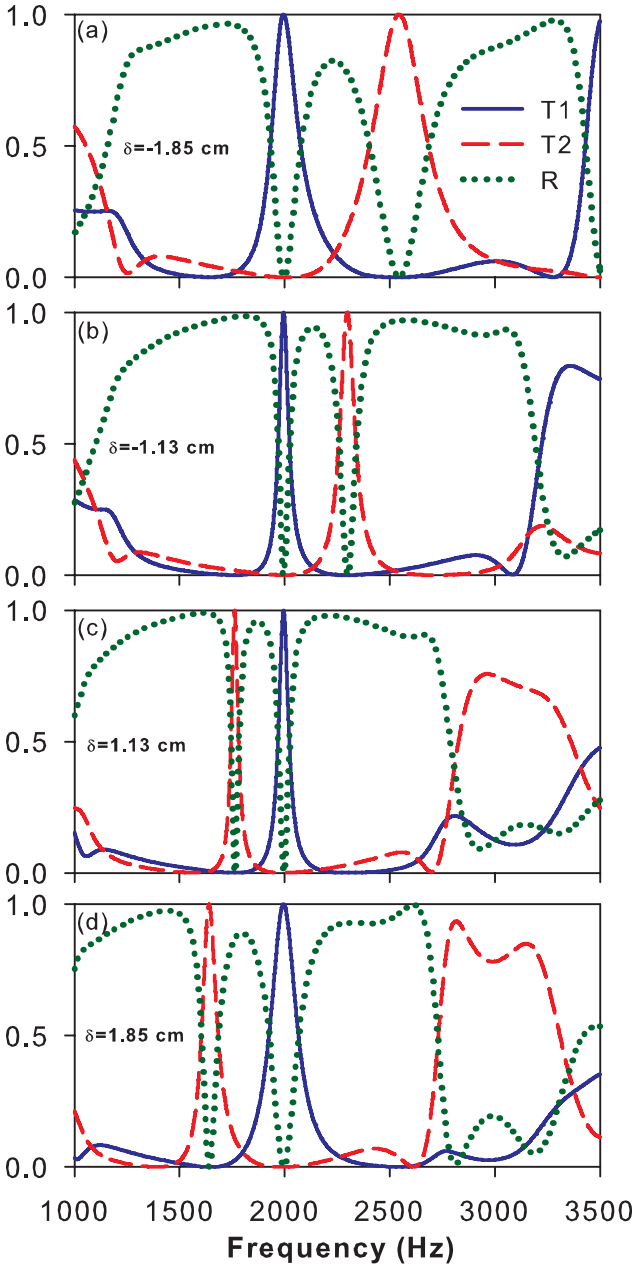

Fig. 8. Variation of the transmission along the output 1 (continuous curve), the output 2 (discontinuous curve) and the reflection in the input (dotted curve) of the demultiplexer as a function of the frequency f for different values of δ and for $d_0 = d_1 + d_2 = 8.57$ cm.

line falls at the same frequency for all δ values, its width decreases as δ decreases and disappears for $\delta = 0$ (Fig. 8), giving rise to bound in continuum states [44]. In addition, the shape and width of the AIT resonance change slightly when δ becomes negative (i.e., for a permutation of both stubs 1 and 2). The position and width of the resonance along the second line strongly depend on δ.

Indeed, as the first AIT resonance has two transmission zeros around $f_0 = 2000$ Hz, the position of the second AIT resonance falls above $f_0 = 2000$ Hz for $\delta < 0$, cross the first resonance at $\delta = 0$ and reappears below $f_0 = 2000$ Hz for $\delta > 0$. This behavior is similar to the one obtained in Figure 3 for the cross-structure where the crossing between the two resonances takes place for $\delta = 0$. Also, the variation of the quality factor Q of the two AIT resonances in the two outputs lines as a function of δ, follows the same behavior as in Figure 4. In particular, Q increases rapidly when the absolute value of δ decreases and tends towards infinity when δ tends to zero.

3.2 Demultiplexer based on Fano resonances

As mentioned in reference [12], in order to achieve a Fano resonance, one should take both stubs with identical lengths, but slightly different from $\frac{d_0}{2}$ (i.e., $d_1 = d_2 \neq d_0/2$) along the first output line. Similarly, we should take $d_3 = d_4 \neq d_0'/2$ along the second output line. The explicit expressions of the eight different lengths d_1, d_2, d_3, d_4, d_5, d_6, d_0 and d_0' should satisfy the following equations in order to obtain a total transmission along one output line keeping the other line unaffected

$$d_1 = d_2 = \frac{d_0}{2} + \varepsilon, \tag{17}$$

$$d_5 = d_2, \tag{18}$$

$$d_3 = d_4 = \frac{d_0}{2} + \frac{\varepsilon}{2}, \tag{19}$$

$$d_0' = d_0 + 3\varepsilon, \tag{20}$$

$$d_6 = d_3 \tag{21}$$

where ε represents the detuning between the lengths of the different guides constituting the demultiplexer. Figure 9 gives the variation of transmission coefficients T_1 and T_2 and reflection coefficient R as a function of the frequency f for different values of ε around $\varepsilon = 0$. From Figure 9 one can see that both resonances are of Fano type that is a resonance near a transmission zero. In addition, both resonances present different asymmetric line shapes (i.e., opposite Fano parameters [1]) in order to achieve a full transmission in one line and no signal in the other line. We can notice that for $\varepsilon = -0.925$ cm for example (Fig. 9a), the transmission along the first output (continuous curve) is unity ($T_1 = 1$) at $f = 1803$ Hz, the transmission along the second output T_2 (discontinuous curve) and the reflection R (dotted curve) vanish (i.e. $T_2 = R = 0$). Similarly, when the transmission along the second line (discontinuous curve) reaches unity ($T_2 = 1$) at $f = 1640$ Hz, the transmission along the first line T_1 (continuous curve) and the reflection R (dashed curve) vanish (i.e., $T_1 = R = 0$). Also, there exists a frequency between the two resonances for which the reflection along the input line reaches almost unity ($R \simeq 1$), while the transmission along the first line T_1 (continuous curve) and the transmission along the second line T_2 (discontinuous curve) vanish (i.e., $T_1 \simeq T_2 \simeq 0$). This behavior does not exist in the case of AIT resonances (Fig. 8). In addition, we can see that for $\varepsilon < 0$, the resonance in the second line falls below the one in the first line (Fig. 9a) and when ε increases both resonances fall close to each other and their widths decrease (Fig. 9b). For $\varepsilon = 0$, both resonances fall at the same frequency (around 2000 Hz),

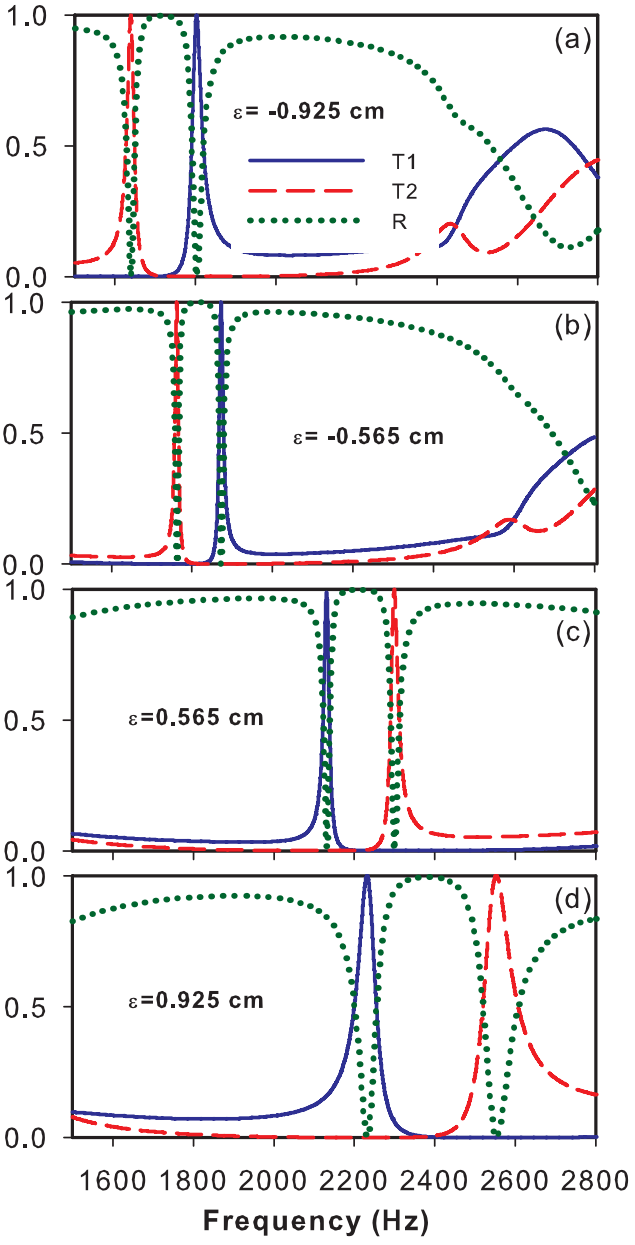

Fig. 9. Variation of the transmission spectra along the output 1 (continuous curve), the output 2 (discontinuous curve) and the reflection in the input (dotted curve) of the demultiplexer as a function of the frequency f for different values of ε and for $d_0 = d_1 + d_2 = 8.57\,\text{cm}$.

their widths vanish giving rise to bound in continuum states [44]. For $\varepsilon > 0$, the resonance in the second line falls above the one in the first line (Fig. 9c); its width increases when ε increases (Fig. 9d). These results are summarized in Figure 10 where we have plotted the frequencies of both resonances as function of ε. We can see that contrary to Figure 3, the frequencies of both Fano resonances depend on ε. Also, the quality factors of the two resonances (not shown here) are almost identical and tend to infinity when ε tends to zero. Finally, the amplitude of the filtered resonances in Figures 8 and 9 can be affected considerably when loss is taken into consideration in particular for narrow resonances as in Figure 5.

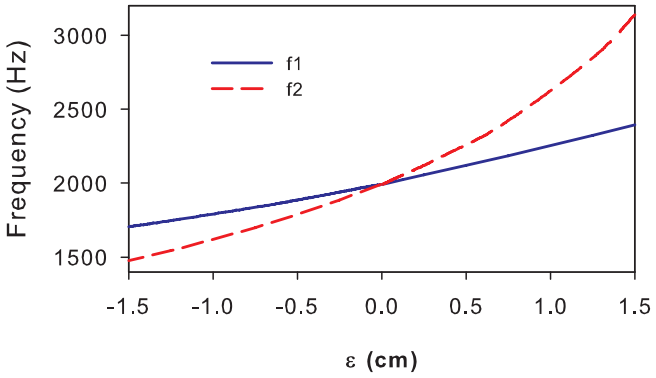

Fig. 10. Variation of the frequencies of the two Fano resonances as a function of ε.

4 Conclusion

In this work we have studied a Y-shaped acoustic demultiplexer based on two different configurations. The first demultiplexer is based on a cross structure, in this case we used the AIT-type resonances presented by such structures to realize a perfect demultiplexing. We have given the analytical expressions of the lengths of the different guides to achieve a total transmittance in one output line canceling at the same time the reflection and transmission in the other lines. By taking into account the loss in the guides, we have shown that the property of demultiplexing still remains valid, however the amplitude of the output signal does not reach unity. In the second configuration we have studied the U-shaped structure for the design of the demultiplexer. In this case, we have shown two possibilities of demultiplexing by using either AIT symmetrical resonances or Fano asymmetrical resonances. In both cases we have determined analytically the expressions of the lengths of the different guides to get the total transmission in one output line keeping the other lines unaffected. For both demultiplexers, we have shown that the frequencies of the filtered resonances as well as their widths (i.e., the quality factors) can be tuned by appropriately choosing the lengths of the different waveguides constituting these systems. The confinement of the filtered and stopped resonances along each line are shown through an analysis of the displacement field. The experimental results predicted in this work can be easily validated by simple experiments in the audible frequency range [13,14,33].

Supplementary Material

Transmission and reflection coefficients for cross and U demultiplexer structures using the Green's function method.

The Supplementary Material is available at https://www.epjap.org/10.1051/epjap/2020190324/olm.

Author contribution statement

A. Mouadili made substantial contribution to analytical and numerical calculation as well as plotting the curves

and writing the original draft of the manuscript. E.H. Boudouti and B. Djafari-Rouhani contribution consists to supervising and writing/correcting the final version of the manuscript.

References

1. U. Fano, Phys. Rev. **124**, 1866 (1961)
2. For a review, see M. Fleischhauer, A. Imamoglu, J.P. Marangos, Rev. Mod. Phys. **77**, 633 (2005)
3. S.E. Harris, Phys. Today **50**, 36 (1997)
4. M. Tomita, K. Totsuka, R. Hanamura, T. Matsumoto, J. Opt. Soc. Am. B **26**, 813 (2009)
5. Y-F Xiao, M. Li, Y-C Liu, Y. Li, X. Sun, Q. Gong, Phys. Rev. A **82**, 065804 (2010)
6. B.-B. Li, Y.-F. Xiao, C.-L. Zou, X.-F. Jiang, Y.-C. Liu, F.-W. Sun, Y. Li, Q. Gong, Appl. Phys. Lett. **100**, 021108 (2012)
7. X. Yang, M. Yu, D.-L. Kwong, C.W. Wong, Phys. Rev. Lett. **102**, 173902 (2009)
8. Y. Sato, Y. Tanaka, J. Upham, Y. Takahashi, T. Asano, S. Noda, Nat. Photon. **6**, 56 (2012)
9. N. Caselli, F. Intonti, F. La China, F. Biccari, F. Riboli, A. Gerardino, L. Li, E.H. Linfield, F. Pagliano, A. Fiore, M. Gurioli, Nat. Commun. **9**, 396 (2018)
10. A. Mouadili, E.H. El Boudouti, A. Soltani, A. Talbi, A. Akjouj, B. Djafari-Rouhani, J. Appl. Phys. **113**, 164101 (2013)
11. A. Mouadili, E.H. El Boudouti, A. Soltani, A. Talbi, B. Djafari-Rouhani, A. Akjouj K. Haddadi, J. Phys.: Condens. Matter **26**, 505901 (2014)
12. E.H. El Boudouti, T. Mrabti, H. Al-Wahsh, B. Djafari-Rouhani, A. Akjouj, L. Dobrzynski, J. Phys.: Condens. Matter **20**, 255212 (2008)
13. A. Santillán, S.I. Bozhevolnyi, Phys. Rev. B **84**, 064304 (2011)
14. A. Merkel, G. Theocharis, O. Richoux, V. Romero-Garcia, V. Pagneux, Appl. Phys. Lett. **107**, 244102 (2015)
15. M. Amin, A. Elayouch, M. Farhat, M. Addouche, A. Khelif, H. Bağci, J. Appl. Phys. **118**, 164901 (2015)
16. Y. Jin, E.H. El Boudouti, Y. Pennec, B. Djafari-Rouhani, J. Phys. D Appl. Phys. **50**, 425304 (2017)
17. F. Zangeneh-Nejad, R. Fleury, Phys. Rev. Lett. **122**, 014301 (2019)
18. I. Quotane, E.H. El Boudouti, B. Djafari-Rouhani, Phys. Rev. B **97**, 024304 (2018)
19. M. Vinod, G. Raghavan, V. Sivasubramanian, Sci. Rep. **8**, 17706 (2018)
20. M. Oudich, B. Djafari-Rouhani, B. Bonello, Y. Pennec, S. Hemaidia, F. Sarry, D. Beyssen, Phys. Rev. Appl. **9**, 034013 (2018)
21. Y. Jin, Y. Pennec, B. Djafari-Rouhani, J. Phys. D **51**, 494004 (2018)
22. B. Luḱyanchuk, N.I. Zheludev, S.A. Maier, N.J. Halas, P. Nordlander, H. Giessen, C.T. Chong, Nat. Mater. **9**, 707 (2010)
23. J. Wu, B. Jin, J. Wan, L. Liang, Y. Zhang, T. Jia, C. Cao, L. Kang, W. Xu, J. Chen, P. Wu, Appl. Phys. Lett. **99**, 161113 (2011)
24. L. Yang, J. Wang, L.Z. Yang, Z.D. Hu, X. Wu, G. Zheng, Sci. Rep. **8**, 2560 (2018)
25. S. Simoncelli, Y. Li, E. Cortes, S.A. Maier, Nano Lett. **18**, 3400 (2018)
26. T. Huang, S. Zeng, X. Zhao, Z. Cheng, P.P. Shum, Photonics **5**, 23 (2018)
27. R. Ghaffarivardavagh, J. Nikolajczyk, S. Anderson, X. Zhang, Phys. Rev. B **99**, 024302 (2019)
28. E. Kamenetskii, A. Sadreev, A. Miroshnichenko, *Fano Resonances in Optics and Microwaves: Physics and Applications* (Springer, Berlin, 2018)
29. For a review, see I. Novikova, R.L. Walsworth, Y. Xiao, Laser Photon. Rev. **6**, 333 (2012) and references therein.
30. C. Liu, Z. Dutton, C.H. Behroozi, L.V. Hau, Nature **409**, 490 (2001)
31. L.V. Hau, S.E. Harris, Z. Dutton, C.H. Behroozi, Nature **397**, 594 (1999)
32. O. Katz, O. Firstenberg, Nat. Commun. **9**, 2074 (2018)
33. H. Long, Y. Cheng, X. Liu, Appl. Phys. Lett. **111**, 143502 (2017)
34. W.M. Robertson, C. Baker, C. Brad Bennett, Am. J. Phys. **72**, 255 (2004)
35. A. Mouadili, E.H. El Boudouti, A. Soltani, A. Talbi, K. Haddadi, A. Akjouj, B. Djafari-Rouhani, J. Phys. D **52**, 075101 (2019)
36. Y. Pennec, B. Djafari-Rouhani, J.O. Vasseur, H. Larabi, A. Khelif, A. Choujaa, S. Benchabane, V. Laude, Appl. Phys. Lett. **87**, 261912 (2005)
37. B. Rostami-Dogolsara, M.K. Moravvej-Farshi, F. Nazari, Phys. Rev. B **93**, 014304 (2016)
38. Y. Pennec, B. Djafari-Rouhani, J.O. Vasseur, A. Khelif, P.A. Deymier, Phys. Rev. E **69**, 046608 (2004)
39. B. Rostami-Dogolsara, M. Kazem Moravvej-Farshi, F. Nazari, J. Mol. Liq. **281**, 100 (2019)
40. O. Richoux, V. Achilleos, G. Theocharis, I. Brouzos, Sci. Rep. **8**, 12328 (2018)
41. X. Zhang, C. Meng, Z. Yang, Sci. Rep. **7**, 13907 (2017)
42. W.M. Robertson, I. Shirk, E. Campbell, AIP Adv. **9**, 035013 (2019)
43. V. Vasseur, A. Akjouj, L. Dobrzynski, B. Djafari-Rouhani, E.H. El Boudouti, Surf. Sci. Rep. **54**, 1 (2004)
44. C.W. Hsu, B. Zhen, A.D. Stone, J.D. Joannopoulos, M. Soljačić, Nat. Rev. Mater. **1**, 16048 (2016)

Cite this article as: Abdelkader Mouadili, El Houssaine El Boudouti, and Bahram Djafari-Rouhani, Acoustic demultiplexer based on Fano and induced transparency resonances in slender tubes, Eur. Phys. J. Appl. Phys. **90**, 10902 (2020)